MIEF2 over-expression promotes tumor growth and metastasis through reprogramming of glucose metabolism in ovarian cancer

Shuhua Zhao
Fourth Military Medical University
Yuan Shi
Fourth Military Medical University
Xiaohong Zhang
Fourth Military Medical University
Lu Cheng
Fourth Military Medical University
Tingting Song
Fourth Military Medical University
Bing Wu
China Medical University Hospital
Jia Li
Fourth Military Medical University
Hong Yang (yanghongdoc@163.com)
Fourth Military Medical University https://orcid.org/0000-0002-5355-0829

Research

Keywords: Mitochondrial elongation factor 2, growth; metastasis, glycolysis; OC

Posted Date: October 29th, 2020

DOI: https://doi.org/10.21203/rs.3.rs-97858/v1

Version of Record: A version of this preprint was published on December 14th, 2020. See the published version at https://doi.org/10.1186/s13046-020-01802-9.

Abstract

Background: Increasing evidence has revealed the close link between mitochondrial dynamic dysfunction and cancer. MIEF2 (mitochondrial elongation factor 2) is mitochondrial outer membrane protein that functions in the regulation of mitochondrial fission. However, the expression, clinical significance and biological functions of MIEF2 are still largely unclear in human cancers, especially in ovarian cancer (OC).

Methods: The expression and clinical significance of MIEF2 were determined by qRT-PCR, western blot and immunohistochemistry analyses in tissues and cell lines of OC. The biological functions of MIEF2 in OC were determined by *in vitro* and *in vivo* cell growth and metastasis assays. Furthermore, the effect of MIEF2 on metabolic reprogramming of OC was determined by metabolomics and glucose metabolism analyses.

Results: MIEF2 expression was significantly increased in OC mainly due to the down-regulation of miR-424-5p, which predictes poor survival for patients with OC. Knockdown of MIEF2 significantly suppressed OC cell growth and metastasis both *in vitro* and *in vivo* by inhibiting G1-S cell transition, epithelial-to -mesenchymal transition (EMT) and inducing cell apoptosis, while forced expression of MIEF2 had the opposite effects. Mechanistically, mitochondrial fragmentation-suppressed cristae formation and thus glucose metabolism switch from oxidative phosphorylation to glycolysis was found to be involved in the promotion of growth and metastasis by MIEF2 in OC cells.

Conclusions: MIEF2 play a critical role in the promotion of OC progression and may serve as a valuable prognostic biomarker and therapeutic target in treatment of this malignancy.

Background

Ovarian cancer (OC) is one of the most common gynecological malignancies in women worldwide [1]. Despite advances of combined therapies including surgery and adjuvant approaches, the prognosis of patients with ovarian cancer continues to be poor. The molecular mechanisms involved in ovarian carcinogenesis are still poorly defined, which limited the effective methods for clinical treatment [2,3]. Accordingly, identification of novel molecular alterations contribute to the metastatic growth of OC cells is crucial for the development of novel diagnostic and therapeutic strategies to obtain more effective treatment in this malignancy.

Alteration of glucose metabolism characterized by increased aerobic glycolysis (also known as Warburg effect) has been well established as one of the hallmarks of cancer[4], which contributes cancer cell growth and metastasis by providing both energy and substrates for biosynthesis[5-7]. Accumulating evidence has revealed mitochondrial dysfunction as one of the most common reason for increased aerobic glycolysis in cancer cells [8-11], suggesting that identification of novel regulators contributing mitochondrial dysfunction may uncover molecular mechanisms underlying the increased aerobic glycolysis and tumor progression.

Mitochondria are crucial organelles involved in cellular metabolism regulation. During the lifetime of a cell, the morphology and function of mitochondrial is continuously remodeled by the balance between fission and fusion events [12-14]. During recent years, the close links between fragmented mitochondrial networks and cancer has been revealed in various types of human cancers[15], including liver[16,17], breast[18,19], lung[20,21] and colon[22] cancers. In addition, abnormal expressions of mitochondria fission and fusion proteins such as DRP1 (dynamin related protein 1) and MFN1 (mitofusion 1) have also been observed. MIEF2 (mitochondrial elongation factor 2) is a mitochondrial outer membrane protein that functions in the regulation of mitochondrial fission [23]. However, the expression, clinical significance and biological functions of MIEF2 is still largely unclear in cancer, especially in ovarian cancer (OC).

In this study, we conducted the first study on MIEF2 in ovarian cancer to clarify its expression pattern, clinical significance, biological effects in this malignancy.

Methods

Cell culture and tissue collection

Human ovarian cancer (OC) cell lines (A2780, SKOV3, OVCAR3, HEY and ES2) and one normal ovarian cell line IOSE80 were purchased from the Cell Bank of Chinese Academy of Sciences (Shanghai, China). All cells were authenticated with the STR profiling test and cultured in Dulbecco's Modified Eagle (DMEM) or RPMI-1640 Medium supplied with 10% fetal bovine serum,100 U/ml penicillin and streptomycin in an incubator with 5% CO2 at 37 °C. In addition, 152-paired tumor and corresponding non-tumor surrounding tissue samples from patients with ovarian cancer (30 for qRT-PCR analysis; 122 for IHC staining analysis) were collected at the First Affiliated Hospital of the Fourth Military Medical University in Xi'an, China. The study was approved by the Ethics Committee of Fourth Military Medical University in Xi'an, China, and performed in compliance with the Declaration of Helsinki of the World Medical Association. Informed consents were obtained from all individuals.

Over-expression and knockdown of target genes

The transient knockdown of MIEF2 in OC cells were obtained with the transfection of small interference RNA (siRNA) using Lipofectamine 2000 (Invitrogen, California, USA) according to the manufacturer's protocol. The sequence si-MIEF2#1 was 5'- ACACCTAAGT

TCAGCACTATAGCAC-3'; The sequence si-MIEF2#2 was 5'- GCCATGCCTTGAAGATGT

GAATAAA-3'. The stable MIEF2 knockdown OC cells were obtained with the shRNA expression vector generated by a pSilencer™ 3.1-H1 puro vector (Ambion, Austin, TX, USA). Synthetic miRNA mimics were purchased from Qiagen. For MIEF2 over-expression, the open reading frame sequence of MIEF2 was amplified and cloned into a pcDNA^{TM}3.1(C) vector (Invitrogen, V790-20). miRNAs mimics (miR-424-5p) and control oligonucleotide (NC) were designed and synthesized by RiboBio Inc (Guangzhou, China) and transfected with Lipofectamine 2000 according to the manufacturer's instructions..

RNA extraction and quantitative real-time PCR (qRT-PCR)

RNA was extracted from OC cells using Trizol reagent (Invitrogen, USA). Then, reverse transcription of extracted RNA was performed using a PrimeScript® RT reagent kit (Takara, Japan) following to the manufacturer's instructions. PCR amplification was performed using SYBR Premix Ex Taq (Takara, Japan). Relative expressions of target genes were calculated using the $2^{-\triangle\triangle Ct}$ method and β-actin was considered as a reference gene for normalization. The primers sequences were listed in the supplementary table 2.

Cells were lysed with RIPA buffer containing a cocktail of protease inhibitors (Sigma, USA). Proteins (35 μg) were separated on 10% SDS-PAGE gels and transferred onto PVDF membrane (Millipore, USA). The membranes were then blocked with 5% milk and probed with primary and secondary horseradish-peroxidase-labeled antibodies. After washing three times, the signaling was detected by an enhanced chemiluminescence detection system (ECL; Amersham Pharmacia Biotech). The antibodies used in the study were listed in the supplementary table 3.

Immunohistochemistry (IHC) analysis

Paraffin-embedded tissue sections (4 μM) were rehydrated, and subsequently blocked with 3% hydrogen peroxide and treated with hot citrate buffer. After that, primary antibodies of MIEF2 and Ki-67 were added to the sections and incubated overnight at 4 °C. The results were determined by an IHC detection kit (MXB, Fuzhou, China) according to the manufacturer's protocol. The IHC staining intensity was scored independently by two observers. Briefly, the scores for the proportion of positive staining (1, <5%; 2, 5-30%; 3, 30-70%; 4, >70%) and staining intensity (0, no staining; 1, weak; 2, moderate; 3, strong) were multiplied for each observer and then averaged..

MTS assay

A total of 1×10^3 OC cells were plated in 96-well cell culture plates (020096, Xinyou Biotech, Hangzhou, China). After grown for 0, 24, 48, 72, 96 and 120 h, 20 μL MTS solution (Promega, G3581) was added to the cells and incubated two hours at 37°C. Finally, the absorption values at 490 nm were measured with a Bio-Rad's microplate reader to determine the relative cellular proliferation capacities.

Colony formation assay

A total of 500 OC cells were seeded in 6-well plates and cultured for 15 days. After that, formed colonies were fixed by 4% paraformaldehyde for 15 min and stained with crystal violet, respectively.

Flow cytometry analysis of cell cycle and cell apoptosis

OC cells were washed with PBS and then analyzed with a cell cycle (F-6012, US Everbright Inc) or an Annexin V (FITC-conjugated) apoptosis (F-6012, US Everbright Inc) kit, respectively, according to their

manufacturer's protocols. Cell cycle distribution in each phase and percentage of apoptotic cells were determined with a flow cytometry (Beckman, Fullerton, CA).

Wound-healing cell migration assay

OC cells were cultured in 6-well plates and grown to 90% confluence. A plastic pipette tip was used for scratching in the bottom of wells. Then, cells were washed two times with the culture medium without fetal bovine serum and images were captured with a light Olympus microscope at 0 and 24 hours. Image J software was used for the determination of relative migration in each group.

Matrigel invasion assay

Matrigel-coated Invasion Chamber (BD Biosciences, UJ, USA) in 24-well dishes was used for assessment of cell invasion. Briefly, 2×10^4 OC cells were seeded in the upper chamber of the transwell insert in serum-free culture medium and cultured for 48 h. Penetrated cells were fixed in 4% paraformaldehyde and stained with 0.5% crystal violet. The number of penetrated cells in each group was counted under a light Olympus microscope.

In vivo tumorigenicity assay

A total of 1×10^7 OC cells with stable MIEF2 knockdown were subcutaneously injected into the flank of 4-5 weeks old male BALB/c athymic nude mice (six mice per group). Tumor volumes were measured every week. Tumors were removed 5 weeks post cells injection and their size and weight were determined. All animal studies were approved by the Institutional Animal Experiment Committee of Xijing hospital and carried out in accordance with the UK Animals (Scientific Procedures) Act, 1986.

In vivo metastatic assay

A total of 5×10^6 OC cells with stable MIEF2 knockdown were intravenously injected into the tail vein of 4-5 weeks old male BALB/c athymic nude mice. After 7 weeks, the mice were sacrificed and metastatic tumors formed in their lungs were determined with hematoxylin and eosin (H&E) staining analysis.

Detection of oxygen consumption rate (OCR) and mitochondrial respiratory chain complexes activities

OC cells were plated into an XF96 plate at a density of 1.0×10^4 /well and cultured overnight. The XF96 Extracellular Flux Analyzer (Seahorse Bioscience) was used for detection of cellular oxygen consumption in OC cells, according to the manufacturer's protocols.

A commercial kit from abcam (ab110419) was used for determination of activities of the five mitochondrial respiratory chain complexes, following to the manufacturer's protocols. The absorption values at 340 nm (complexes I and V), 550 nm (complexes III and IV) and 600 nm (complex II) was measured with a Bio-Rad's microplate reader, respectively.

ATP Measurements

ATP production was determined with ATP Determination Kit (Thermo Fisher Scientific, A22066) following to the manufacturer's instruction. Briefly, OC cells with different treatment were homogenized in the lysis buffer. The results were determined by luminescence (Promega, Glomax 20/20 luminometer) and normalized to protein concentration.

Determination of glucose consumption and lactate production

Glucose colorimetric and a lactate assay kit purchased from Nanjing jiancheng Bioengineering institute (Nanjing, China) were used for determination of lactate production/glucose concentrations before and after 24 h cell culture in OC cells, following to their manufacturer's protocols. In addition, a pH meter (PB-11 Basic Meter, The Netherlands) was used for the measurement of pH value in cell culture medium.

Statistical analysis

Data were presented as mean ± SEM. The SPSS software (17.0 version) was used for statistical analysis and $p<0.05$ was considered as statistically significant (*). The two-tailed student's t-test or one-way ANOVA with Tukey's post-hoc test was used for comparison between two or multiple groups, respectively. Kaplan-Meier method and log-rank test were used for overall survival and recurrence-free survival analysis.

Results

MIEF2 expression is increased in tumor tissues and cell lines of OC and associated with poor prognosis in patients with OC.

The expression of MIEF2 was firstly evaluated in tumor and corresponding peritumor tissues from 30 patients with ovarian cancer (OC) using quantitative real-time PCR (qRT-PCR) analysis. Our results showed a significantly up-regulated MIEF2 in OC tissues when compared with peritumor tissues (Fig. 1A). Consistently, increased MIEF2 expression was also detected in five OC cell lines (A2780, SKOV3, OVCAR3, HEY and ES2) compared with normal ovarian cell line IOSE80 (Fig. 1B-1C).

To explore the correlation between MIEF2 expression and survival of patients with OC, immunohistochemical (IHC) analysis was applied for MIEF2 protein expression in another 122-paired OC tumor and peritumor tissues. MIEF2 was significantly higher in tumor tissues of OC compared to peritumor tissues (Fig. 1D). Kaplan-Meier survival analysis demonstrated that OC patients with higher MIEF2 expression had obvious poorer overall survival compared to MIEF2 lower expression patients (Fig. 1E). Consistently with this, bioinformatics analysis using the KM plotter [24] also indicated that OC patients with high MIEF2 expression had significant shorter overall survival (P= 0.001) and progression free survival (Figure 1F). Taken together, MIEF2 expression was up-regulated in OC cells/tissues and associated with poor prognosis for patients with OC.

Knockdown of MIEF2 suppressed OC cell growth through induction of G1-S cell cycle arrest and cell apoptosis.

Increased MIEF2 expression implied that MIEF2 may function as an oncogene in the tumorigenesis of OC. To prove this, MIEF2 expression was knocked-down in OVCAR3 and ES2 cells (Fig 2A and 2B) with relatively high MIEF2 expression shown in Fig 1D and Fig 1F. Knockdown of MIEF2 significantly suppressed cell proliferation and colony formation in OVCAR3 and ES2 cells (Fig 2C and 2D), as determined by MTS cell viability and colony formation assays. Suppressed cell growth might be caused by decreased cell proliferation or increased cell apoptosis, or both. To characterize the mechanism by which MIEF2 knockdown suppressed OC cell growth, the effects of MIEF2 knockdown on cell proliferation and apoptosis were determined by flow cytometry cell cycle distribution, EdU (5-ethynyl-2'-deoxyuridine) incorporation and flow cytometry cell apoptosis assays. As shown in Fig. 2E-2G, knockdown of MIEF2 in OVCAR3 and ES2 cells resulted in a significant cell cycle arrest at G1 phase (Fig. 2E), a lower percentage of proliferating cells (Fig. 2F), as well as a significant reduction of cell apoptosis (Fig. 2G), suggesting that MIEF2 knockdown suppressed OC cell growth through induction of G1-S cell cycle arrest and cell apoptosis.

MIEF2 knockdown suppressed migration and invasion of OC cells

The effects of MIEF2 knockdown on cell migration and invasion of OC cells was further explored. Knockdown of MIEF2 significantly suppressed the migration abilities of OVCAR3 and ES2 cells compared to control cells (Fig. 3A), as evidenced by wound healing assay. In addition, MIEF2 knockdown also suppressed the invasion abilities of OVCAR3 and ES2 cells, as shown by transwell matrigel invasion assay (Fig. 3B). Previous studies have shown that epithelial-mesenchymal-transition (EMT) plays crucial roles during metastasis of malignant tumors through decreasing cell-cell contact and increasing migration and invasion[25]. To investigate how MIEF2 controls OC migration and invasion, the expressions of principal epithelial and mesenchymal regulators were determined by qRT-PCR and Western blot analysis. MIEF2 knockdown significantly enhanced the levels of epithelial regulators of E-cadherin and ZO-1, while decreased the levels of mesenchymal regulators of N-cadherin and Vimentin (Fig 3C and 3D), indicating that MIEF2 knockdown suppressed migration and invasion of OC through inhibiting EMT.

MIEF2 knockdown suppressed OC growth and metastasis in nude mice

We then explored the *in vivo* tumor-promoting effects of MIEF2 in OC. Stably MIEF2 knockdown (shMIEF1) and control (shCtrl) OVCAR3 cells (Fig. S1A and S1B) were injected into the flanks of nude mice to construct xenograft models. MIEF2 knockdown significantly inhibited the growth of tumors (Fig 4A) and decreased their weights (Fig 4B) in OVCAR3 tumor-bearing mice. Immunochemistry (IHC) staining showed significantly decreased MIEF2 expression in shMIEF2 xenograft tumor tissues compared to those from shCtrl, implying that the tumor growth inhibiting effect was exerted by MIEF2 knockdown (Fig. 4C). In line with the *in vitro* results, significantly fewer proliferating and more apoptotic cells were detected in xenografts from shMIEF2 group compared to shCtrl group, as indicated by Ki-67 and TUNEL

staining assays, respectively (Fig. 4D and 4E). In addition, MIEF2 knockdown also significantly suppressed lung metastasis of OVCAR3 cells in nude mice (Fig. 4F).

Over-expression of MIEF2 enhanced OC cell growth and metastasis

To provide further support for the promoting effects of MIEF2 on cell growth and metastasis in OC, MIEF2 was over-expressed in SKOV3 and HEY cells with relatively low MIEF2 expression shown in Fig 1F and Fig 1E. Over-expression of MIEF2 expression (Fig. 5A and 5B) markedly increased the viability and colony formation capacities of SKOV3 and HEY cells (Fig. 5C and 5D). In addition, forced expression of MIEF2 also obviously enhanced the migration and invasion abilities of SKOV3 and HEY cells (Fig. 5E and 5F).

MIEF2 over-expression is mainly mediated by down-regulation of miR-424-5p in OC.

MicroRNAs (miRNAs) are important post-transcriptional regulators of gene expression. To identify potential miRNAs contribute to MIEF2 over-expression in OC, target prediction was applied using microRNA Data Integration Portal (mirDIP)[26]. Among the top six predicted miRNAs targeting MIEF2 (Fig. S2), only miR-424-5p transfection decreased MIEF2 expression in SKOV3 and HEY cells (Fig. 6A and 6B). In addition, a significant negative correlation was observed between the levels of miR-424-5p and MIEF2 in tumor tissues from 30 patients with OC (Fig. 6C). As expected, a significantly decreased miR-424-5p was observed in tumor tissues of OC compared to the normal counterparts from 30 OC patients (Fig. 6D), indicating that MIEF2 over-expression is mainly mediated by down-regulation of miR-424-5p in OC. Furthermore, we found that forced expression of miR-424-5p (Fig. 6E-6G) significantly attenuated the promoting effects of MIEF2 over-expression on OC growth and metastasis (Fig. 6H and 6I).

MIEF2 enhanced the Warburg effect of ovarian cancer cells

Mitochondrial plays critical roles in the regulation of cellular metabolism. Considering that MIEF2 is a crucial regulator of mitochondrial fission and morphology, we hypnotized that MIEF2 over-expression may contribute to the reprogramming of metabolism in OC cells. To define the metabolic alterations induced by MIEF2, we first examined the effects of MIEF2 knockdown and over-expression on mitochondrial oxygen consumption rate (OCR), oxidative phosphorylation (OXPHOS) activity and ATP production. Our results showed that knockdown of MIEF2 in OVCAR3 cells significantly increased the rate of oxygen consumption (Fig. 7A), activities of the respiratory chain complexes I-V (Fig. 7B) and ATP production (Fig. 7C), while forced MIEF2 expression exhibited an opposite effects in SKOV3 cells (Fig. 7A-7C). Electron microscopy showed that MIEF2 significantly induced mitochondrial fragmentation with increased cristae width (Fig. 7D), a phenotype consistent with mitochondrial OXPHOS defects [27]. These results suggest that MIEF2 suppressed mitochondrial respiration in OC cells mainly through mitochondrial fragmentation suppressed cristae formation. Considering that impaired mitochondrial OXPHOS is often accompanied by increased glycolysis, which has been well-known as the “Warburg effect”, we accordingly assessed the potential role of MIEF2 in the glycolysis of OC cell. Glucose consumption and lactate production assays revealed that MIEF2 knockdown significantly suppressed glucose consumption and lactate production, whilst pH value in the culture medium was significantly

increased. In contrast, MIEF2 over-expression exhibited the opposite effects (Fig 7E-7G). To further corroborate these results, we performed relative quantification of cellular metabolites using gas chromatography-mass spectrometry (GC-MS) analysis. We found that MIEF2 knockdown resulted in a significant decrease in intracellular concentrations of glycolytic intermediates (glucose 6-phosphate (G6P), fructose 6-phosphate (F6P), glyceraldehyde 3-phosphate (GA3P), 3-phosphoglycerate (3PG) and lactate), while a significant increase in TCA cycle metabolites (citrate, aconitate, α-ketoglutarate, fumarate, malate) in OVCAR3 cells, as determined by gas chromatography-mass spectrometry (GC-MS) analysis. In contrast, over-expression of MIEF2 was associated with increased glycolytic intermediates, while decreased TCA cycle metabolites in SKOV3 cells (Fig. 7H). These results indicate that MIEF2 switched the glucose metabolism of OC cells from oxidative phosphorylation to glycolysis in OC cells.

MIEF2 promoted OC growth and metastasis through activating aerobic glycolysis.

Increased aerobic glycolysis has been coupled with various malignant phenotypes of cancer cells, including tumor growth and metastasis [7,28]. To test whether the promoting effects of MIEF2 on OC cell growth and metastasis were dependent on the increased aerobic glycolysis, glucose in cell culture medium was replaced by galactose, which cannot be fermented, requiring cells to rely on mitochondrial metabolism to generate sufficient ATP for survival. As shown in Fig 8A-8D, inhibition of glycolysis by galactose significantly attenuated the growth and metastasis of SKOV3 and HEY cells promoted by MIEF2 over-expression, as determined by MTS cell viability, colony formation, wound healing and transwell matrigel invasion assays, implying that MIEF2 exerts its oncogenic functions in OC cells through activating aerobic glycolysis.

Discussion

Mitochondria are the primary energy source for cellular functions, such as survival, proliferation, and migration [29, 30]. The morphology of mitochondrial is dynamically regulated by the balance between fusion and fission events to maintain energy and metabolic homeostasis[12]. During recent years, a series of studies have revealed the close links between the unbalanced mitochondrial dynamics and various human cancers[15], including liver[16, 17], breast[18, 19], lung[20, 21] and colon[22] cancers. MIEF2 (mitochondrial elongation factor 2) is a outer mitochondrial membrane protein involved in the regulation of mitochondrial fission [23]. However, the expression, clinical significance and biological functions of MIEF2 is still largely unclear in cancer, especially in ovarian cancer (OC). Here, we for the first time demonstrate that MIEF2 is frequently over-expressed in tissue and cell lines of OC mainly due to the down-regulation of miR-424-5p, and over-expression of MIEF2 is significantly associated with poor survival for patients with OC. Consistent with our present findings about MIEF2 in OC, increased expressions of mitochondrial dynamic proteins such as DRP1 (dynamin related protein 1), mitofusin 1 (MFN1) and mitofusin 2 (MFN2) have also been reported in human cancers of liver[16], lung[21, 31], colon[32] and breast[19]. Moreover, significant correlations between the abnormal expressions of mitochondrial dynamic proteins of DRP1 and MFN1 and the prognosis of patients have also been

reported in liver [16] and lung cancer. In OC, another critical crucial mitochondrial fission factor MARCH5 has also been reported to substantially up-regulated in tumor tissue in comparison with the normal control [33]. These studies collectively indicate that mitochondrial dynamic dysfunction plays critical roles in the progression of human cancers.

Elevated expression levels of MIEF2 suggest that MIEF2 may play an oncogenic role in the progression of OC. With this connection, the biological functions of MIEF2 in OC cells were explored both *in vitro* and *in vivo*. We found that MIEF2 knockdown markedly suppressed the viability and colony formation abilities of OVCAR3 and ES2 cells, while forced expression of MIEF2 significantly increased viability and colony formation abilities of SKOV3 and HEY cells. Furthermore, subcutaneous xenograft models confirmed that knockdown of MIEF2 significantly attenuated tumorigenicity of OC cells in nude mice. Similarly, over-expression of another mitochondrial fission factor DRP1 has also been shown to promote tumor cell growth in human cancers of liver[16], lung[21] and breast[34]. Moreover, we found that the mechanism by which MIEF2 suppressed OC cell growth was mediated by inducing both G1–S cell cycle arrest and cell apoptosis. In line with this, Ki-67 and TUNEL staining assays also indicated fewer proliferating cells and more apoptotic cells in MIEF2 knockdown subcutaneous tumors compared to corresponding controls.

In addition to the functions of MIEF2 in tumor growth, its roles in metastasis were also investigated in OC cells. Knockdown of MIEF2 in OVCAR3 and ES2 cells significantly suppressed their migration and invasion abilities. Conversely, overexpression of MIEF2 enhanced the migration and invasion abilities in SKOV3 and HEY cells. In OC, increased expression of another mitochondrial fission regulator MARCH5 has also been shown to promote migration and invasion *in vitro* and *in vivo* [33]. Furthermore, we found that the molecular mechanism by which MIEF2 exerts its metastatic promoting effect was mediated by inducing epithelial-mesenchymal transition (EMT). Consistently, a previous study in hepatocellular carcinoma also indicated that silencing of another mitochondrial fission protein MTP18 also suppressed the invasion ability of pancreatic cancer cell through inhibiting EMT[35]. In contrast, mitochondrial fusion protein MFN1 has been shown to play an suppressive role in the EMT of HCC cells [36].

MicroRNAs (miRNAs) are important post-transcriptional regulators of gene expression. MiR-424-5p has been established as a novel tumor suppressor that was frequently down-regulated in several types of cancer, including breast cancer[37], hepatocellular carcinoma[38], bladder cancer[39] and cervical cancer[40]. A previous study in ovarian cancer also has reported that MiR-424-5p was significantly down-regulated and promoted cell proliferation [41]. Consistently, our present study also revealed a significant down-regulation of miR-424-5p in OC cells. Furthermore, we demonstrated that down-regulation of miR-424-5p contributed to OC cell growth and metastasis through up-regulating MIEF. However, we still cannot rule out the possibility that other genetic or epigenetic alterations may also contribute to the overexpression of MIEF2 in OC.

Reprogrammed glucose metabolism characterized by preferential dependence on glycolysis for energy production (also known as Warburg effect), even in the presence of oxygen, has been well known as a

hallmark of cancer[4]. Although several oncogenes such as myc and RAS have been shown to play important roles in this metabolic reprogramming[42], the key plays contribute increased aerobic glycolysis in cancer cells still needs further investigation. Glucose metabolism in cancer is balanced by glycolysis and mitochondrial oxidative phosphorylation (OXPHOS)[43]. During the past several decades, mitochondrial malfunction has been revealed as one of the most common reason for increased aerobic glycolysis in cancer cells [10, 21]. However, identification of novel regulators contributing mitochondrial dysfunction and thus increased aerobic glycolysis is still urgently needed. Here, we revealed that over-expression of MIEF2 in OC cells significantly promoted the Warburg effect characterized by metabolic switch from oxidative phosphorylation to glycolysis. Furthermore, we found that the enhanced aerobic glycolysis in OC was involved in MIEF2-promoted tumor growth and metastasis. These results suggest that mitochondrial dysfunction play a crucial role in the reprogramming of glucose metabolism and subsequently the progression of human cancers.

Conclusions

In summary, we show for the first time that MIEF2 is commonly over-expressed in OC tissues, and its over-expression is associated with worse survival for patients with OC. MIEF2 plays a crucial oncogenic role in the progression of OC through reprogramming glucose metabolism from oxidative phosphorylation to glycolysis, indicating MIEF2 as a novel prognostic marker and therapeutic target in treatment of this malignancy.

List Of Abbreviations

OC, ovarian cancer; MIEF2, mitochondrial elongation factor 2; qRT-PCR, quantitative real-time PCR ; IHC, immunohistochemistry; DRP1, dynamin related protein 1, MFN1, mitofusion 1; siRNA, small interference RNA; PVDF, polyvinylidene fluoride; SDS-PAGE H&E, hematoxylin and eosin; OCR, xygen consumption rate; OXPHOS, oxidative phosphorylation; ATP, Adenosine triphosphate; GC-MS, gas chromatography-mass spectrometry; TCA cycle, tricarboxylic acid cycle; TUNEL, terminal deoxynucleotidyl transferase-mediated dUTP-biotin nick end labeling; EMT, Epithelial-mesenchymal transition;

Declarations

Ethics approval and consent to participate

A total of 152-paired tumor and corresponding non-tumor surrounding tissue samples from patients with ovarian cancer (30 for qRT-PCR analysis; 122 for IHC staining analysis) were collected at the First Affiliated Hospital of the Fourth Military Medical University in Xi'an, China. The study was approved by the Ethics Committee of Fourth Military Medical University in Xi'an, China, and performed in compliance with the Declaration of Helsinki of the World Medical Association. Informed consents were obtained from all individuals.

All animal studies in nude mice were approved by the Institutional Animal Experiment Committee of Xijing hospital and carried out in accordance with the UK Animals (Scientific Procedures) Act, 1986.

Consent for publication

Not applicable

Availability of data and materials

The datasets used and/or analysed during the current study are available from the corresponding author on reasonable request.

Competing interests

No financial and non-financial competing interests exist in this study.

Funding

This work was supported by the National Major Scientific Instrument and Equipment Development Project of China (Grant No. 2018YFF01012100), the Scientific and Technological Project of Social Development in Shaanxi Province (Grant No. 2016SF-254), the Booster programs of Xijing Hospital (Grant Nos. XJZT19H03, XJZT18MJ92, XJZT19D08, XJZT19ML25).

Author contributions

S.Z. and Y.S. performed most experiments, analyzed data; L.C., T.S. and B.W. participated in the in vitro and vivo study. J.L. and H.Y. designed the overall study, supervised the experiments. J.L. wrote the paper. H.Y. revised the paper and acquired the funding. All authors read and approved the final manuscript.

Acknowledgements

We would like to thank Dr. Jing Zhao, Experimental Teaching Center of Basic Medicine, Fourth Military Medical University for guidance with xenograft studies.

References

[1] Lheureux S, Gourley C, Vergote I, et al. Epithelial ovarian cancer [J]. Lancet, 2019,393(10177):1240-1253.

[2] Lheureux S, Braunstein M, Oza AM. Epithelial ovarian cancer: Evolution of management in the era of precision medicine [J]. CA Cancer J Clin, 2019,69(4):280-304.

[3] Krzystyniak J, Ceppi L, Dizon DS, et al. Epithelial ovarian cancer: The molecular genetics of epithelial ovarian cancer [J]. Ann Oncol, 2016,27 Suppl 1(i4-i10.

[4] Schwartz L, Supuran CT, Alfarouk KO. The warburg effect and the hallmarks of cancer [J]. Anticancer Agents Med Chem, 2017,17(2):164-170.

[5] Kato Y, Maeda T, Suzuki A, et al. Cancer metabolism: New insights into classic characteristics [J]. The Japanese dental science review, 2018,54(1):8-21.

[6] Ganapathy-Kanniappan S, Geschwind JF. Tumor glycolysis as a target for cancer therapy: Progress and prospects [J]. Molecular cancer, 2013,12(152.

[7] Corbet C, Feron O. Tumour acidosis: From the passenger to the driver's seat [J]. Nat Rev Cancer, 2017,17(10):577-593.

[8] Porporato PE, Filigheddu N, Pedro JMB, et al. Mitochondrial metabolism and cancer [J]. Cell research, 2018,28(3):265-280.

[9] Herst PM, Grasso C, Berridge MV. Metabolic reprogramming of mitochondrial respiration in metastatic cancer [J]. Cancer Metastasis Rev, 2018,37(4):643-653.

[10] Lu J, Tan M, Cai Q. The warburg effect in tumor progression: Mitochondrial oxidative metabolism as an anti-metastasis mechanism [J]. Cancer Lett, 2015,356(2 Pt A):156-164.

[11] Corbet C, Feron O. Cancer cell metabolism and mitochondria: Nutrient plasticity for tca cycle fueling [J]. Biochim Biophys Acta Rev Cancer, 2017,1868(1):7-15.

[12] Westermann B. Mitochondrial fusion and fission in cell life and death [J]. Nat Rev Mol Cell Biol, 2010,11(12):872-884.

[13] Lee H, Yoon Y. Mitochondrial fission and fusion [J]. Biochem Soc Trans, 2016,44(6):1725-1735.

[14] Tilokani L, Nagashima S, Paupe V, et al. Mitochondrial dynamics: Overview of molecular mechanisms [J]. Essays Biochem, 2018,62(3):341-360.

[15] Trotta AP, Chipuk JE. Mitochondrial dynamics as regulators of cancer biology [J]. Cell Mol Life Sci, 2017,74(11):1999-2017.

[16] Huang Q, Zhan L, Cao H, et al. Increased mitochondrial fission promotes autophagy and hepatocellular carcinoma cell survival through the ros-modulated coordinated regulation of the nfkb and tp53 pathways [J]. Autophagy, 2016,12(6):999-1014.

[17] Li J, Huang Q, Long X, et al. Mitochondrial elongation-mediated glucose metabolism reprogramming is essential for tumour cell survival during energy stress [J]. Oncogene, 2017,36(34):4901-4912.

[18] Chen L, Zhang J, Lyu Z, et al. Positive feedback loop between mitochondrial fission and notch signaling promotes survivin-mediated survival of tnbc cells [J]. Cell Death Dis, 2018,9(11):1050.

[19] Zhao J, Zhang J, Yu M, et al. Mitochondrial dynamics regulates migration and invasion of breast cancer cells [J]. Oncogene, 2013,32(40):4814-4824.

[20] Qi M, Dai D, Liu J, et al. Aim2 promotes the development of non-small cell lung cancer by modulating mitochondrial dynamics [J]. Oncogene, 2020,39(13):2707-2723.

[21] Rehman J, Zhang HJ, Toth PT, et al. Inhibition of mitochondrial fission prevents cell cycle progression in lung cancer [J]. FASEB J, 2012,26(5):2175-2186.

[22] Tailor D, Hahm ER, Kale RK, et al. Sodium butyrate induces drp1-mediated mitochondrial fusion and apoptosis in human colorectal cancer cells [J]. Mitochondrion, 2014,16(55-64.

[23] Liu T, Yu R, Jin SB, et al. The mitochondrial elongation factors mief1 and mief2 exert partially distinct functions in mitochondrial dynamics [J]. Exp Cell Res, 2013,319(18):2893-2904.

[24] Nagy A, Lanczky A, Menyhart O, et al. Validation of mirna prognostic power in hepatocellular carcinoma using expression data of independent datasets [J]. Scientific reports, 2018,8(1):9227.

[25] Dongre A, Weinberg RA. New insights into the mechanisms of epithelial-mesenchymal transition and implications for cancer [J]. Nat Rev Mol Cell Biol, 2019,20(2):69-84.

[26] Shirdel EA, Xie W, Mak TW, et al. Navigating the micronome–using multiple microrna prediction databases to identify signalling pathway-associated micrornas [J]. PloS one, 2011,6(2):e17429.

[27] Buck MD, O'Sullivan D, Klein Geltink RI, et al. Mitochondrial dynamics controls t cell fate through metabolic programming [J]. Cell, 2016,166(1):63-76.

[28] Lunt SY, Vander Heiden MG. Aerobic glycolysis: Meeting the metabolic requirements of cell proliferation [J]. Annual review of cell and developmental biology, 2011,27(441-464.

[29] Giacomello M, Pyakurel A, Glytsou C, et al. The cell biology of mitochondrial membrane dynamics [J]. Nature reviews Molecular cell biology, 2020,21(4):204-224.

[30] Kim HK, Noh YH, Nilius B, et al. Current and upcoming mitochondrial targets for cancer therapy [J]. Semin Cancer Biol, 2017,47(154-167.

[31] Yu L, Xiao Z, Tu H, et al. The expression and prognostic significance of drp1 in lung cancer: A bioinformatics analysis and immunohistochemistry [J]. Medicine (Baltimore), 2019,98(48):e18228.

[32] Kim YY, Yun SH, Yun J. Downregulation of drp1, a fission regulator, is associated with human lung and colon cancers [J]. Acta Biochim Biophys Sin (Shanghai), 2018,50(2):209-215.

[33] Hu J, Meng Y, Zhang Z, et al. March5 rna promotes autophagy, migration, and invasion of ovarian cancer cells [J]. Autophagy, 2017,13(2):333-344.

[34] Tang Q, Liu W, Zhang Q, et al. Dynamin-related protein 1-mediated mitochondrial fission contributes to ir-783-induced apoptosis in human breast cancer cells [J]. J Cell Mol Med, 2018,22(9):4474-4485.

[35] Zhang Y, Li H, Chang H, et al. Mtp18 overexpression contributes to tumor growth and metastasis and associates with poor survival in hepatocellular carcinoma [J]. Cell death & disease, 2018,9(10):956.

[36] Zhang Z, Li TE, Chen M, et al. Mfn1-dependent alteration of mitochondrial dynamics drives hepatocellular carcinoma metastasis by glucose metabolic reprogramming [J]. Br J Cancer, 2020,122(2):209-220.

[37] Wang J, Wang S, Zhou J, et al. Mir-424-5p regulates cell proliferation, migration and invasion by targeting doublecortin-like kinase 1 in basal-like breast cancer [J]. Biomed Pharmacother, 2018,102(147-152.

[38] Du H, Xu Q, Xiao S, et al. Microrna-424-5p acts as a potential biomarker and inhibits proliferation and invasion in hepatocellular carcinoma by targeting trim29 [J]. Life Sci, 2019,224(1-11.

[39] Matsushita R, Seki N, Chiyomaru T, et al. Tumour-suppressive microrna-144-5p directly targets ccne1/2 as potential prognostic markers in bladder cancer [J]. Br J Cancer, 2015,113(2):282-289.

[40] Zhou Y, An Q, Guo RX, et al. Mir424-5p functions as an anti-oncogene in cervical cancer cell growth by targeting kdm5b via the notch signaling pathway [J]. Life Sci, 2017,171(9-15.

[41] Liu J, Gu Z, Tang Y, et al. Tumour-suppressive microrna-424-5p directly targets ccne1 as potential prognostic markers in epithelial ovarian cancer [J]. Cell Cycle, 2018,17(3):309-318.

[42] Mikawa T, ME LL, Takaori-Kondo A, et al. Dysregulated glycolysis as an oncogenic event [J]. Cell Mol Life Sci, 2015,72(10):1881-1892.

[43] Jose C, Bellance N, Rossignol R. Choosing between glycolysis and oxidative phosphorylation: A tumor's dilemma? [J]. Biochim Biophys Acta, 2011,1807(6):552-561.

Figures

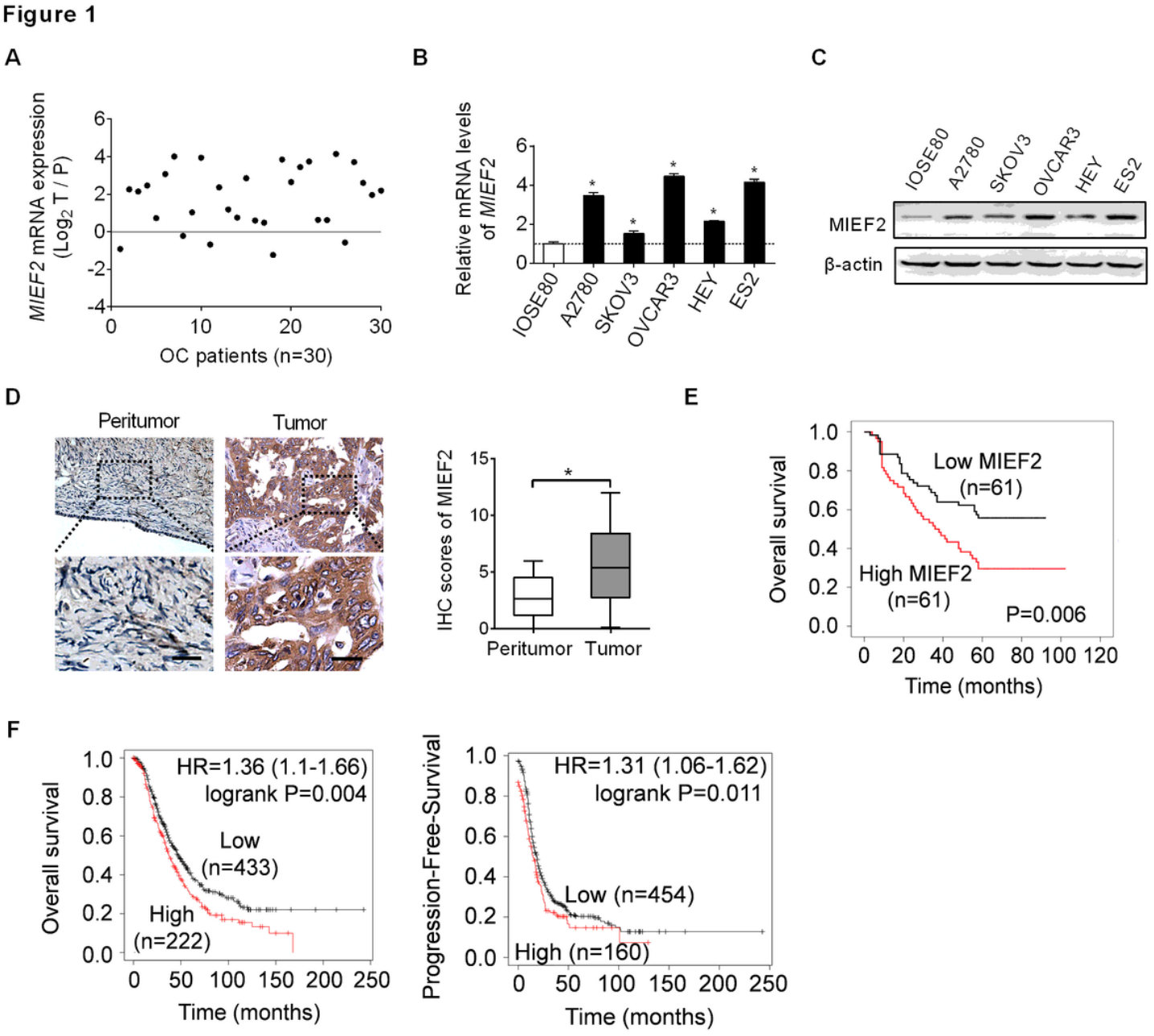

Figure 1

MIEF2 expression is increased in tumor tissues and cell lines of OC and associated with poor prognosis in patients with OC. (A) The expression of MIEF2 in OC was firstly evaluated using qRT-PCR analysis of MIEF2 in paired tumor and peritumor tissues from 30 OC patients. (T, tumor; P, peritumor). (B and C) qRT-PCR and Western blot analysis of MIEF2 expression in five human OC cell lines (A2780, SKOV3, OVCAR3, HEY and ES2) and one normal ovarian cell line IOSE80. (D) Immunohistochemical (IHC) staining of the MIEF2 expression in 122-paired OC tumor and peritumor tissues. Scale bar, 50 μm. (E) Kaplan–Meier plot of overall survival in 122 OC patients with relatively higher or lower MIEF2 expression levels determined

by IHC staining. (F) Bioinformatics analysis using the KM plotter for prognostic significance of MIEF2 in OC patients. *P< 0.05.

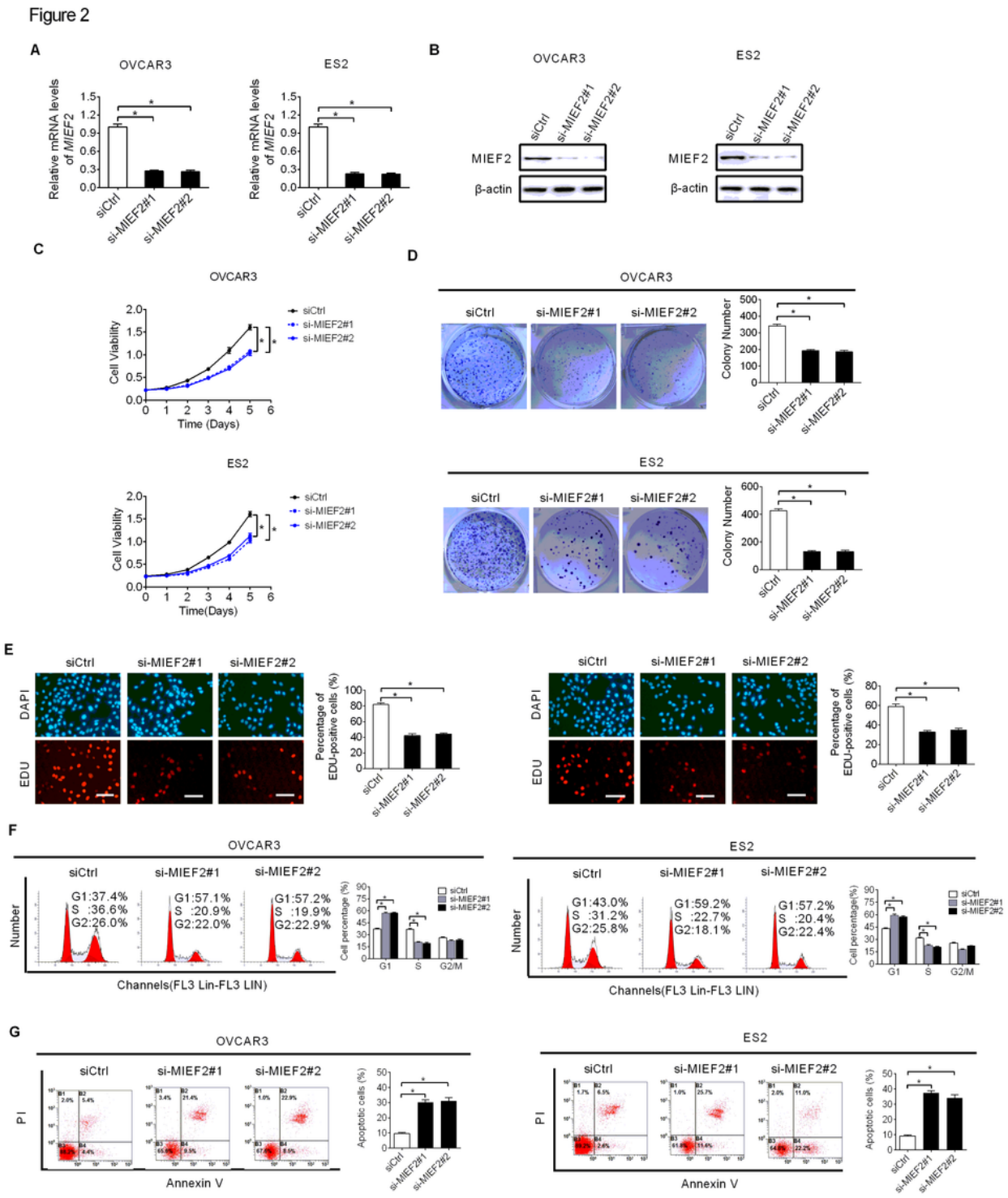

Figure 2

Knockdown of MIEF2 suppressed cell proliferation and cell cycle progression and inhibited cell apoptosis in OC cells. (A and B) Knockdown of MIEF2 was confirmed by qRT-PCR and Western blot analysis in OVCAR3 and ES2 cells. siMIEF2, siRNA against MIEF2; siCtrl, control siRNA. (C and D) MTS cell viability

and colony formation assays in OVCAR3 and ES2 cells with or without MIEF2 knockdown. (E) EdU incorporation assay was performed in in OVCAR3 and ES2 cells with or without MIEF2 knockdown.. Scale bars, 50 μm. (F and G) Flow cytometry analysis for cell cycle distribution and cell apoptosis in OVCAR3 and ES2 cells with or without MIEF2 knockdown. *P< 0.05.

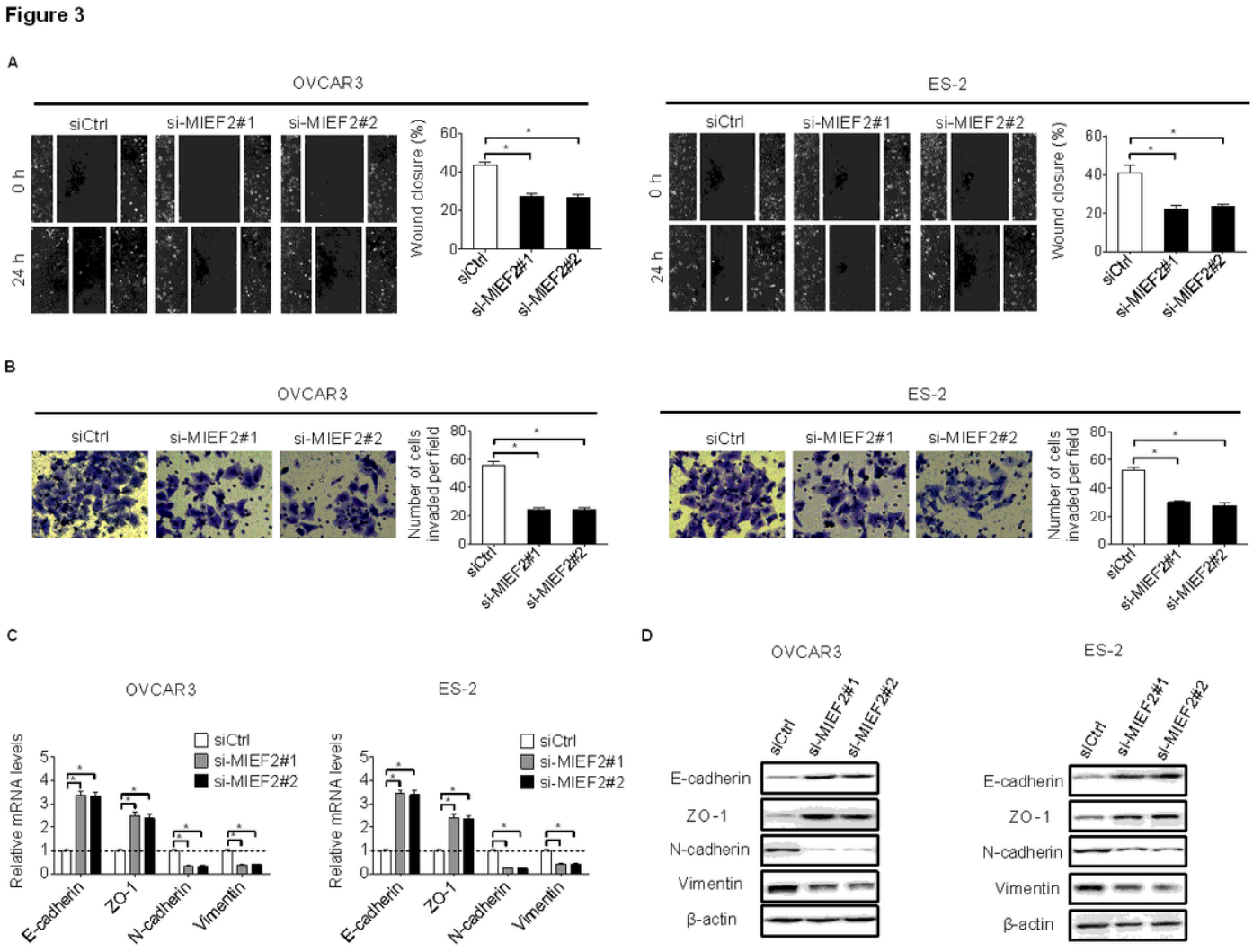

Figure 3

MIEF2 knockdown suppressed migration and invasion of OC cells. (A and B) Scratch wound healing and transwell matrigel invasion assays were applied in OVCAR3 and ES2 cells with or without MIEF2 knockdown. siMIEF2, siRNA against MIEF2; siCtrl, control siRNA. (C and D) qRT- PCR and western blot analysis for expression of epithelial markers of E-cadherin and ZO-1, and mesenchymal markers of N-cadherin and Vimentin in OVCAR3 and ES2 cells with or without MIEF2 knockdown. *P< 0.05.

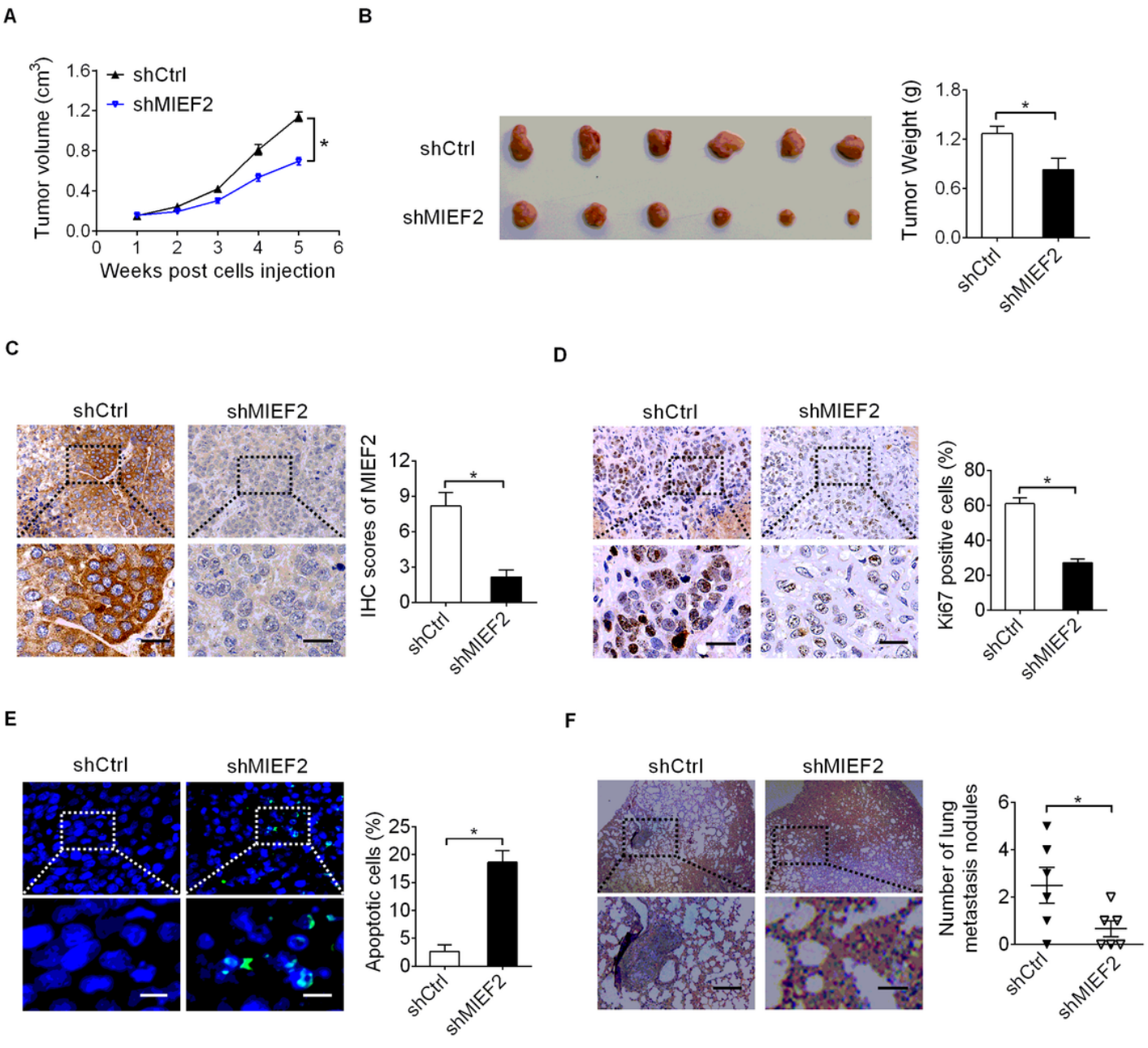

Figure 4

MIEF2 knockdown suppressed OC growth and metastasis in nude mice. (A and B) Growth curves and weights of xenograft tumor developed from OVCAR3 cells with (shMIEF2) or without (shCtrl) MIEF2 knockdown. Scale bars, 20 μm. (C and D) IHC staining of MIEF2 and Ki-67 in xenograft tumors developed from OVCAR3 cells with or without MIEF2 knockdown. Scale bars, 20 μm. (E) TUNEL assay for apoptosis in tumor tissues developed from OVCAR3 cells with or without MIEF2 knockdown. Scale bars, 5 μm. (F) Incidence of lung metastasis in tumor tumors developed from OVCAR3 cells with or without MIEF2 knockdown. Scale bars, 10 μm. *P< 0.05.

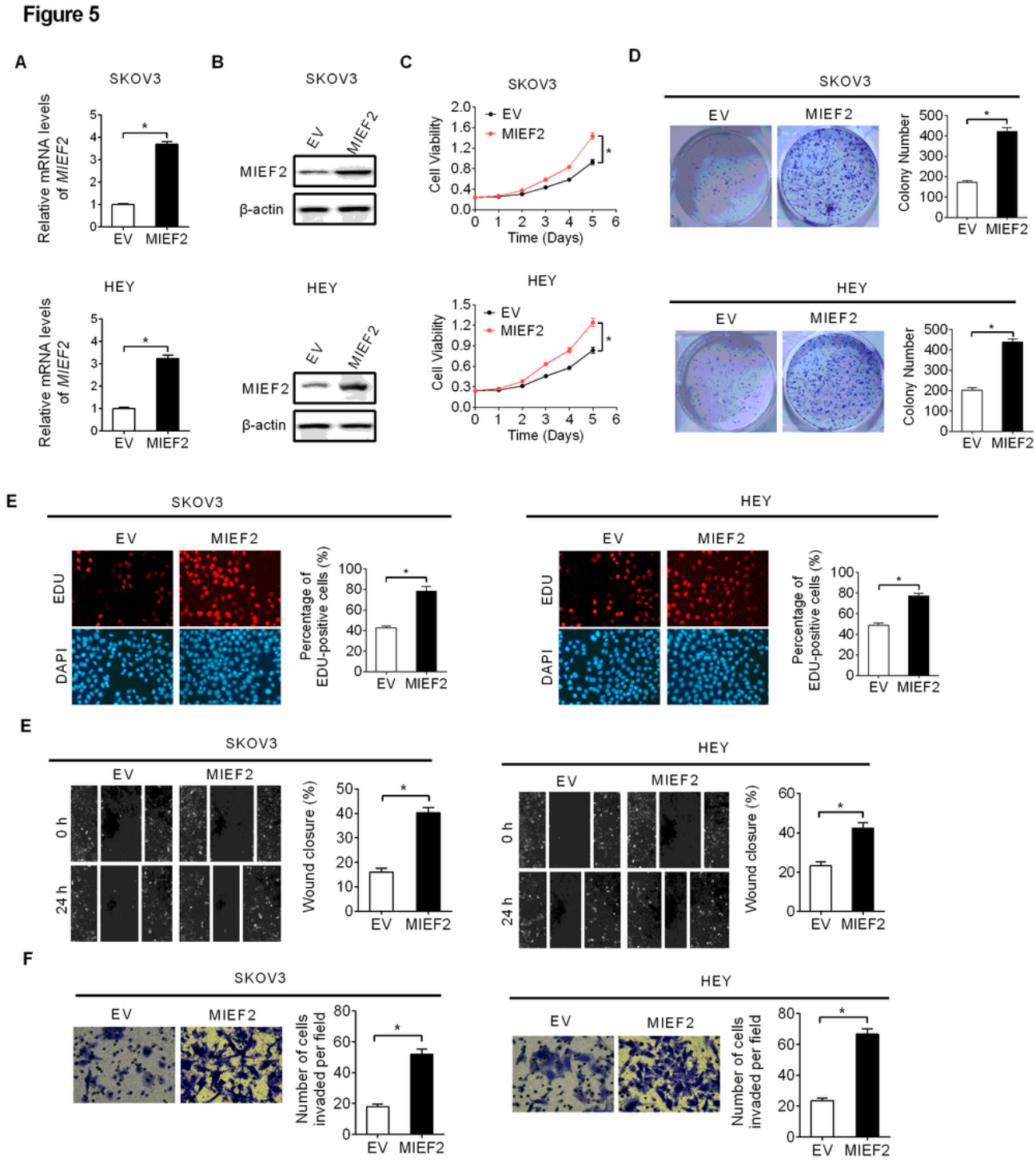

Figure 5

Overexpression of MIEF2 enhanced OC cell growth and metastasis. (A and B) qRT-PCR and western blot analysis for the expression of MIEF2 in SKOV3 and HEY cells with or without MIEF2 overexpression. MIEF2, MIEF2 expression vector; EV, empty vector. (C and D) MTS cell viability and colony formation assays in SKOV3 and HEY cells with or without MIEF2 overexpression. (E and F) Wound healing

migration and transwell matrigel invasion assays in SKOV3 and HEY cells with or without MIEF2 overexpression. *P< 0.05.

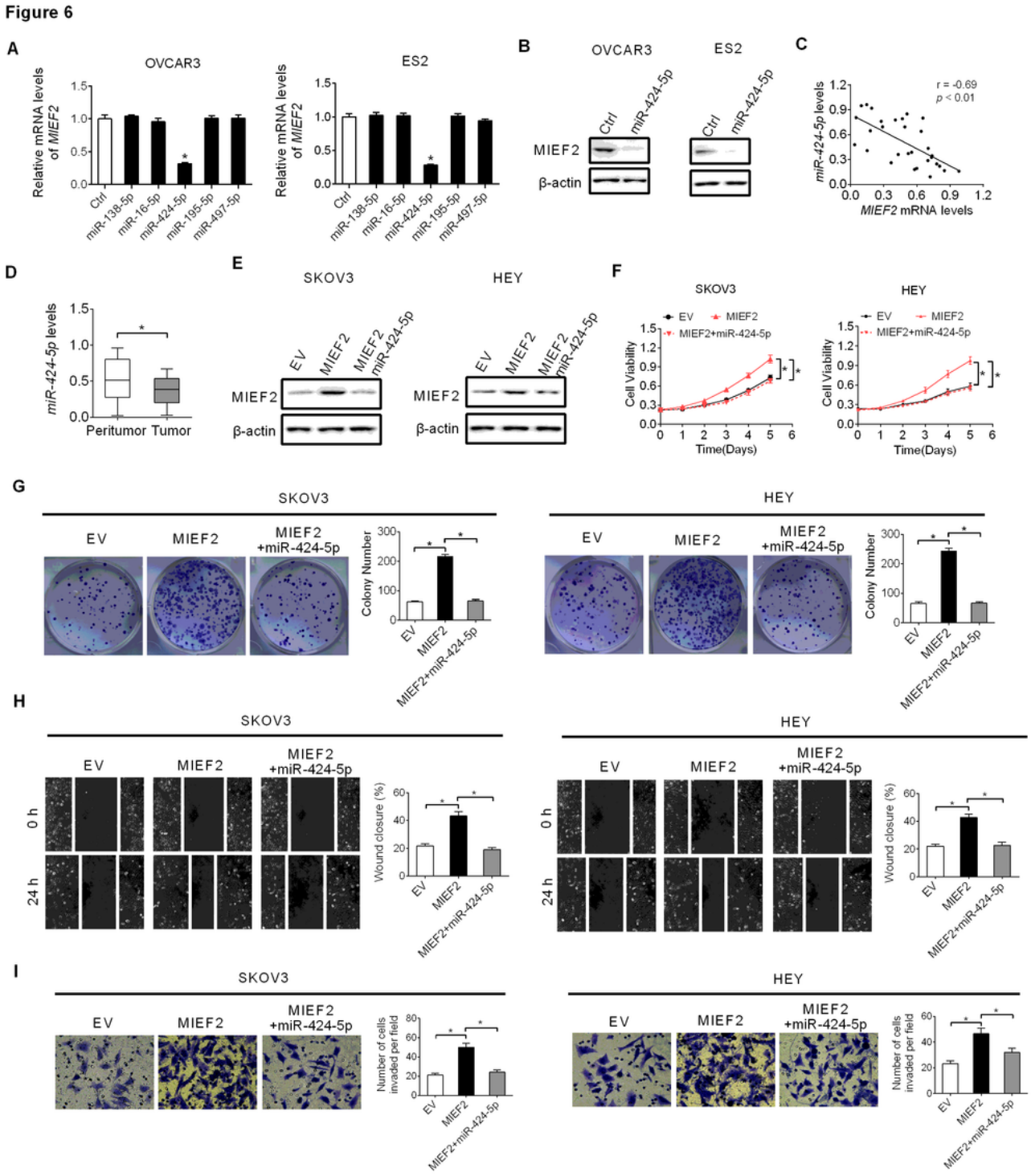

Figure 6

MIEF2 over-expression is mainly mediated by down-regulation of miR-424-5p in OC. (A and B) qRT-PCR and western blot analysis for the expression of MIEF2 in OVCAR3 and ES2 cells after transfection with synthetic miR-424-5p. (C) Correlation between the expression of MIEF2 and miR-424-5p in tumor tissues

from 30 OC patients. (D) The expression of miR-424-5p was determined by qRT-PCR analysis in paired tumor and peritumor tissues from 30 OC patients. (E) The expression of MIEF2 was determined by Western blot analysis in SKOV3 and HEY cells transfected with indicated vectors. (F and G) MTS cell viability and colony formation assays in SKOV3 and HEY cells transfected with indicated vectors. (H and I) Wound-healing and matrigel invasion assays in SKOV3 and HEY cells transfected with indicated vectors. *P< 0.05.

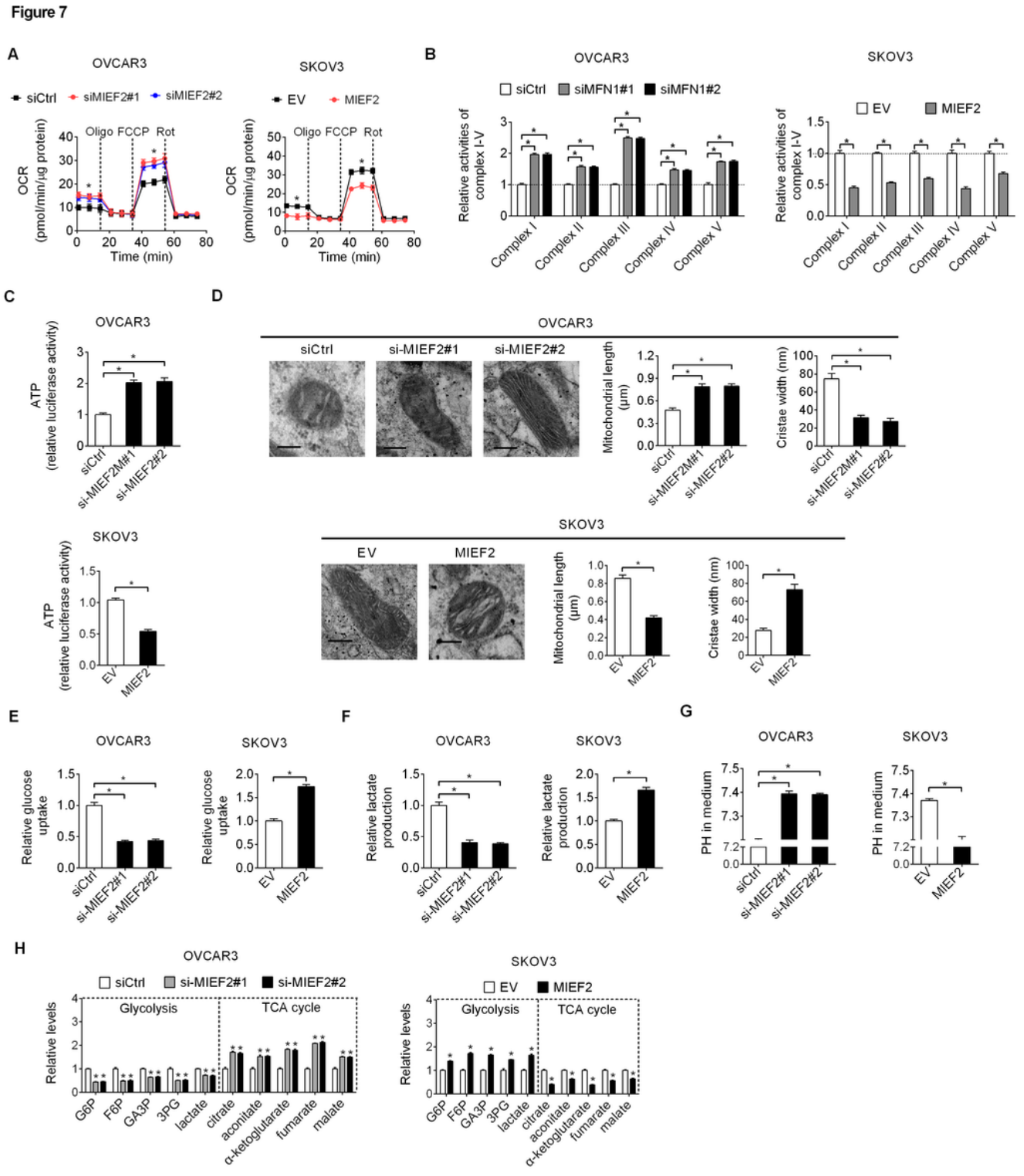

Figure 7

MIEF2 enhanced the Warburg effect of ovarian cancer cells. (A) Oxygen consumption rate (OCR) was determined in OVCAR3 and SKOV3 cells with MIEF2 knocked-down or over-expressed. (B) Relative activities of respiratory complexes I, II, III, IV and V were determined in OVCAR3 and SKOV3 cells with MIEF2 knocked-down or over-expressed. (C) ATP production was measured in OVCAR3 and SKOV3 cells with MIEF2 knocked-down or over-expressed. (D) Representative transmission electron microscopy images of mitochondria in OC cells with treatment as indicated. Scale bars, 0.2 μm. Mitochondrial length and cristae width were quantitatively analyzed. (E and F) Relative glucose consumption and lactate production were determined in OVCAR3 and SKOV3 cells with MIEF2 knocked-down or over-expressed. (G) PH values in cell culture medium were determined in OVCAR3 and SKOV3 cells with MIEF2 knocked-down or over-expressed. (H) Relative intracellular levels of intermediates in glycolysis and TCA cycle were determined by the gas chromatography–time of flight–mass spectrometry (GC-MS) in OVCAR3 and SKOV3 cells with MIEF2 knocked-down or over-expressed. *P< 0.05.

Figure 8

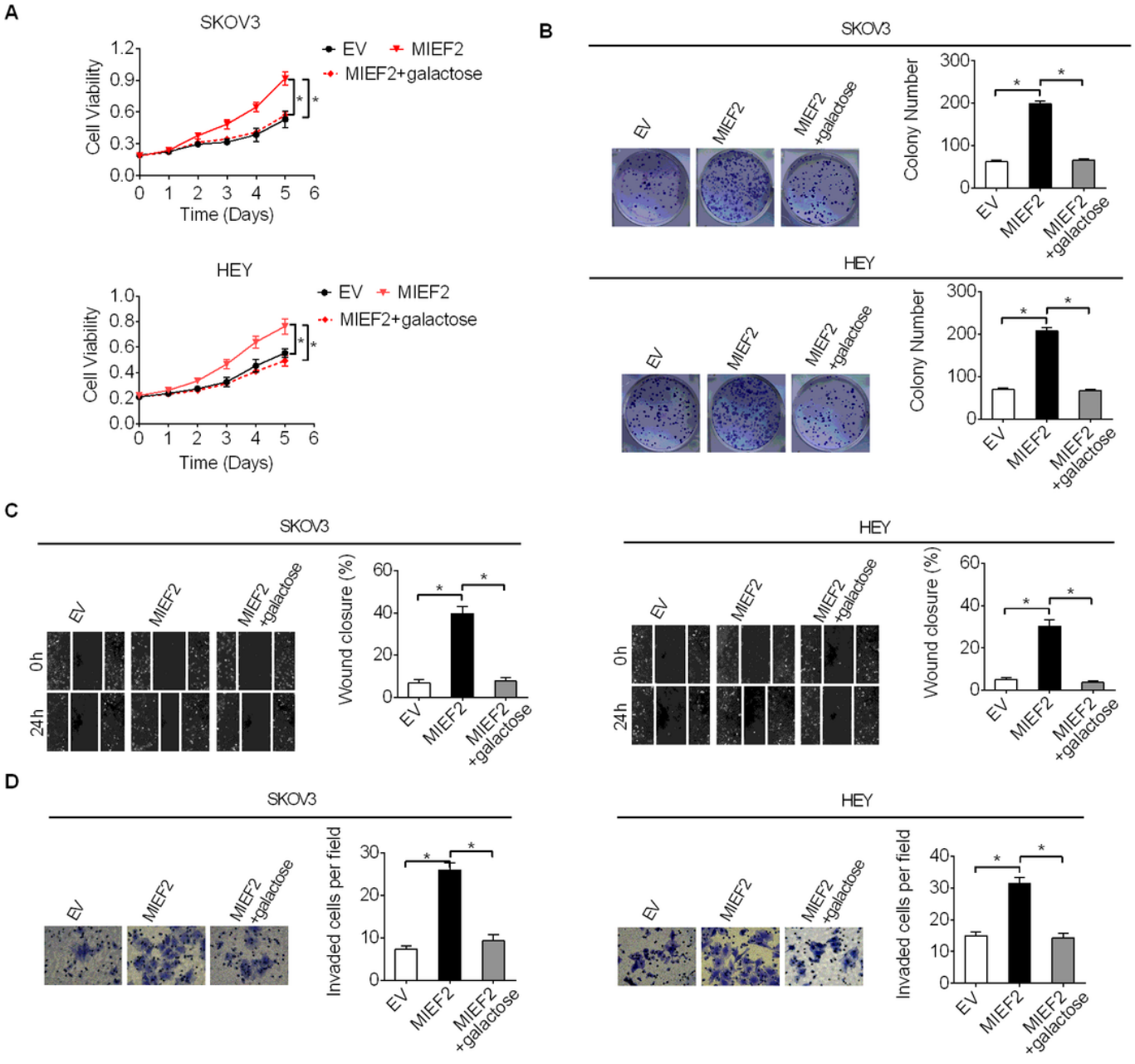

Figure 8

MIEF2 promoted OC growth and metastasis through activating aerobic glycolysis. (A and B) MTS cell viability and colony formation assays were performed in SKOV3 and HEY cells treated with or without galactose to suppress glycolysis. (C and D) Wound-healing and matrigel invasion analysis were performed in SKOV3 and HEY cells treated with or without galactose to suppress glycolysis. *P< 0.05.

Supplementary Files

This is a list of supplementary files associated with this preprint. Click to download.

- supplementaryfiguresandtables.docx